

DOI 10.1007/s11595-016-1514-5

Thermodynamic and Kinetic Studies of Effective Adsorption of 2,4,6-trichlorophenol onto Calcined Mg/Al-CO₃ Layered Double Hydroxide

ZHANG Dan¹, ZHAO Guoqing, YU Jingang, YAN Tao, ZHU Mingyue, JIAO Feipeng*
(College of Chemistry and Chemical Engineering, Central South University, Changsha 410083, China)

Abstract: Adsorption of 2, 4, 6-trichlorophenol (TCP) onto the calcined Mg/Al-CO₃ layered double hydroxide (CLDH) was investigated. The prepared Mg/Al-CO₃ layered double hydroxide (LDH) and CLDH were characterized by powder X-ray diffraction (XRD) and thermo gravimetric analyzer-differential scanning calorimeters (TG-DSC). Moreover, 2,4,6-trichlorophenol (TCP) was removed effectively (94.7% of removal percentage in 9 h) under the optimized experimental conditions. The adsorption kinetics data fitted the pseudo-second-order model well. The Freundlich, Langmuir, and Tempkin adsorption models were applied to the experimental equilibrium adsorption data at different temperatures of solution. The adsorption data fitted the Freundlich adsorption isotherm with good values of the correlation coefficient. A mechanism of the adsorption process is proposed according to the intraparticle diffusion model, which indicates that the overall rate of adsorption can be described as three steps.

Key words: 2,4,6-trichlorophenol; calcined Mg/Al-CO₃ layered double hydroxide; adsorption isotherm; thermodynamic; kinetics

1 Introduction

Chlorinated phenolic compounds are widely used as synthetic intermediates in industry and biocides in agriculture or wood preservation^[1]. The 2,4,6-trichlorophenol (TCP) has attracted extensive environmental interest due to its toxicity and persistence in the environment. TCP is a widespread environmental pollutant in soil, surface water and groundwater. The concentration of TCP has been found up to 1.96 g/L in the chlorinated drinking water^[2,3]. In order to remove TCP from aqueous solutions, various treatment technologies have been applied, such as adsorption technology using the multi-walled carbon nanotubes removed Cu (II)^[4] and the activated carbons generated from various sources such as oil palm shell^[5], biological treatment^[6] and photochemical treatment^[7,8]. The adsorption technique particularly has

gained significant popularity considering its simplicity, versatility and potentiality for regeneration^[3,9], which is one of the important procedures for the removal of TCP from the wastewater. Among many adsorbents, a class of anionic clays known as layered double hydroxides (LDHs) have proved to be effective adsorbents for the removal of various anionic pollutants.

The general formula of LDHs is $[MII_{1-x}MIII_x(OH)_2]^{x+}(A^{n-})_{x/n} \cdot mH_2O$, where M^{II} is a divalent metal cation (Mg²⁺, Zn²⁺, Cu²⁺, etc), and M^{III} is a trivalent metal cation (Al³⁺, Cr³⁺, Fe³⁺, etc) that occupies octahedral sites in the hydroxide layers; Aⁿ⁻ is an exchangeable interlayer anion; and x is defined as the ratio of M^{III}/(M^{II}+M^{III}) that determines the layer charge density^[10]. The calcination of LDH containing carbonate as interlayer anion has a memory effect^[11]. This effect makes the formation of MIIMIIIO solid solution in the CLDH capable of recovering the LDH layered structure upon treatment with water or aqueous solution containing various anions.

The removal of TCP by CLDH has rarely been reported recently in the literatures. The goal of our study was to investigate the adsorption capacity of TCP on CLDH in aqueous medium via various adsorption parameters such as pH, initial TCP concentration and

©Wuhan University of Technology and SpringerVerlag Berlin Heidelberg 2016

(Received: Dec. 10, 2015; Accepted: Mar. 4, 2016)

ZHANG Dan(张丹):E-mail:1152163260@qq.com

*Corresponding author: JIAO Feipeng(焦飞鹏): Prof.; Ph D;

E-mail: jiaofp@163.com

Funded by the National Natural Science Foundation of China (No.21476269)

temperature. The equilibrium isotherm and kinetic models for the adsorption process were also studied to evaluate the viability and effectiveness of this process. Based on the intraparticle diffusion model, the adsorption mechanism was also discussed.

2 Experimental

2.1 Materials

2,4,6-Trichlorophenol ($C_6H_3Cl_3O$, 98% purity), supplied by Aladdin Chemistry Co. Ltd. was used without any further purification. $ZnCl_2 \cdot 6H_2O$, $AlCl_3 \cdot 6H_2O$, NaOH and Na_2CO_3 were purchased from Beijing Chemical Co. Ltd.

2.2 Preparation of CLDH

Mg/Al- CO_3 LDH was prepared by the co-precipitation method. A mixed solution of $MgCl_2 \cdot 6H_2O$ (0.15 mol) and $AlCl_3 \cdot 6H_2O$ (0.05 mol) in 150.0 mL of deionized water was added to 150 mL of the alkali solution containing NaOH (0.45 mol) and Na_2CO_3 (0.15 mol) with vigorous stirring during the whole process of addition. During the co-precipitation process, the pH value of the mixed solution was maintained slightly higher than 9 with NaOH solution (0.1 mM). The obtained suspension was submitted to the hydrothermal treatment at 80 °C for 24 h, and then centrifuged, washed with deionized water and dried at 80 °C overnight. CLDH was prepared by calcining LDH in a muffle furnace at the designated temperature of 500 °C for 5 h.

2.3 Characterization

The LDH precursor and CLDH materials before and after the adsorption of TCP were characterized by several techniques. The powder X-ray diffraction (XRD) patterns were recorded on a powder X-ray diffractometer (Rigaku Rint 6000), using Ni-filtered Cu/K α ($\lambda=1.5406\text{\AA}$) radiation at voltage 40 kV and current 250 mA. The samples were scanned in steps of 0.04° (2 θ) in the range of 3°-70° with a count time of 4 s per step. Thermal gravimetric analysis DSC-TG measurements were conducted on a STA449C thermal analyzer under air atmosphere at a heating rate of 10 °C/min from 25 °C to 800 °C. The measurements for the reconstructed LDH were made after TCP removal of 94.7% by CLDH with adsorbent dose 3 g/L, at temperature 25 °C and initial pH 5.2 for 24 h.

2.4 Adsorption experiments

A temperature-controlled shaker bath (tolerance: ± 0.5 °C) was used for the equilibrium studies. The adsorption experiments were carried out in 250 mL

sealed conical flasks. The flasks were placed in the shaker bath immediately after mixing a 50.0 mL TCP solution of appropriate concentration with the prearranged amount of CLDH. Two milliliter of samples were extracted at selected time intervals, separated by filtration and conserved in the vial for latter detection. The pH of each solution was measured with a digital pH meter (Model pHs-3C).

Concentrations of TCP were analyzed by a UV-9600 spectrophotometer, and the absorbance was measured at 294 nm^[11]. The quantity of TCP adsorbed by 1.0 g CLDH at time t , q_t was calculated using the following equation:

$$q_t = \frac{(C_0 - C_e)V}{m} \quad (1)$$

The removal efficiency was measured by the percentage removal of TCP, which was denoted by another equation:

$$\text{Percentage removal(\%)} = \frac{C_0 - C_e}{C_0} \times 100\% \quad (2)$$

where, q_t is the adsorption amount at any time t (mg/g), C_0 and C_e are the initial concentration and equilibrium concentration of the TCP in solution (mg/L), respectively.

3 Results and discussion

3.1 XRD analysis

The XRD pattern of the synthesized LDH was observed that the more intense peaks were located at lower 2θ while less intense lines were present at higher 2θ values, which corresponds to a hydroxalite phase. The sharpness of the (003) and (006) peaks demonstrates the well-crystallized LDH and layered structure of the samples, and similar results have been also reported in the literature^[12]. After calcination, the (003) and (006) reflections essentially disappeared, indicating that the structure of LDH was destroyed and the stacking of the layers became disordered. Only a few diffused peaks were observed, which are attributed to MgO. After TCP adsorption at the concentration of 50 mg·L⁻¹, the re-appearance of (003) and (006) reflections confirmed the “memory effect” of the LDH precursor by the reconstruction to its original LDH structure. Even though these peaks were broadened and the intensity decreased because of some reduction in crystallinity followed by the calcination and rehydration, there are no significant

changes in the interlayer space compared to those of the original LDH matrixes. This unchanged “gallery height” indicates that the intercalation of TCP into the interlayer did not occur, and TCP molecules may be adsorbed onto the surface of the absorbent. To verify the external surface adsorption, the XRD pattern of the reconstructed LDH (RLDH) obtained under the N_2 atmosphere using the CO_2 -free deionized water is shown in Fig.1. It can be observed that the LDH, which was restored from CO_2 -free TCP solution, exhibited the reduction in peaks intensity. However, an insignificant shift in the interlayer spacing suggests that it is difficult to intercalate TCP molecules into the interlayer even in the CO_2 -free water. And the low concentration of CO_3^{2-} in the CO_2 -removed water caused the reduction in peak intensity and increase in peak width, indicating the lower crystallinity. Therefore, TCP has a very weak affinity for CLDH and its intercalation is difficult.

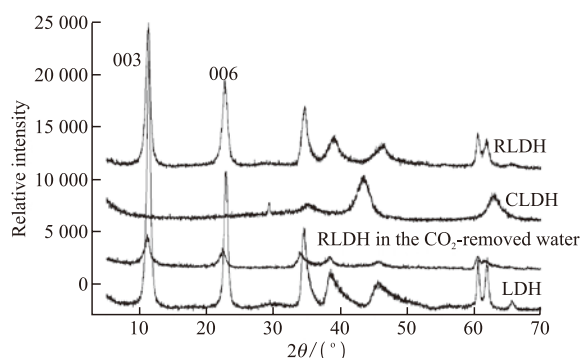


Fig.1 The XRD patterns of LDH, reconstructed LDH in the CO_2 -removed water, Mg/Al-CLDH and RLDH

3.2 TG-DSC analysis

The TG-DSC curves for LDH and RLDH are illustrated in Fig.2. The TG-DSC curve for LDH Fig.2 (a) shows three distinct weight losses in the temperature ranges 0-220 °C, 220-500 °C and 500-800 °C, and the percentage of weight loss is 8.57%, 8.14%, and 2.34 %, respectively. The first weight loss is due to the loss of water cointercalated with carbonates in the hydrotalcite phases and the condensation water, with a small endothermic effect at 120 °C. The second weight loss involves the dehydroxylation of the layers and loss of volatile species (CO_3^{2-}) arising from the interlayer anions. The final mass loss that occurs at higher than 460 °C can be due to the continuous dehydroxylation and decarbonation and the formation of oxide metals. However, the TG curve for the RLDH at $C_i = 50 \text{ mg}\cdot\text{L}^{-1}$ of TCP in Fig.2(b) shows two weight losses. The first one, up to 320 °C, corresponds to the removal of water

physisorbed on the external surface of the crystallinity as well as the water intercalated in the interlayer galleries and corresponds to up to 17.13% of the total weight of the sample. The second step, occurred between 320 °C and 800 °C, presents a significant weight loss of 29.41% with a large endothermic effect at 455 °C, which is assigned to the dehydroxylation of the material as well as the decomposition of TCP. It is worth mentioning that the temperature at which the maximum rate of heat consumption occurred for the second degradation process was higher than that of the LDH, indicating the stronger bonding of the TCP anions.

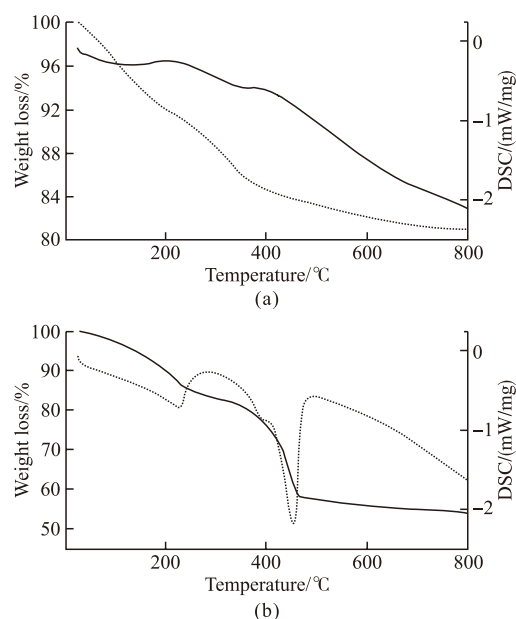


Fig.2 TG-DSC curves for (a) LDH and (b) reconstructed LDH

3.3 Effect of Mg/Al ratio

Taking the important role of Mg in the adsorption into account, we studied the influence of molar ratio of Mg/Al on its removal activity, which is shown in Fig.3. The CLDH samples with different Mg/Al ratios are denoted as Mg_nAl , where n is the molar ratio of Mg^{2+}/Al^{3+} employed in the synthesized mixture. It was found that the removal of TCP by the Mg_3Al reached 94%, compared to 30% and 64% by the samples with Mg_2Al and Mg_4Al , respectively. This phenomenon can be explained by the increase of the specific surface area^[13] and the decrease of the layer charge^[14] with the increase of the molar ratio of Mg^{2+}/Al^{3+} . Mg_4Al represents the highest specific surface area, which improves the surface adsorption. Since the behavior of Mg_3Al sample was better than that of Mg_2Al and Mg_4Al , the detailed investigation was performed only on the Mg_3Al sample.

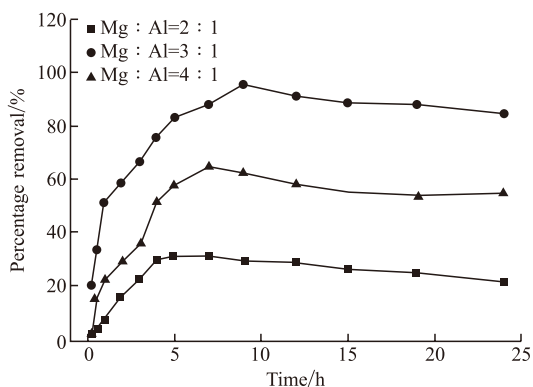


Fig.3 Effect of Mg/Al ratio on TCP removal by CLDH

3.4 Effect of contact time and initial TCP concentration

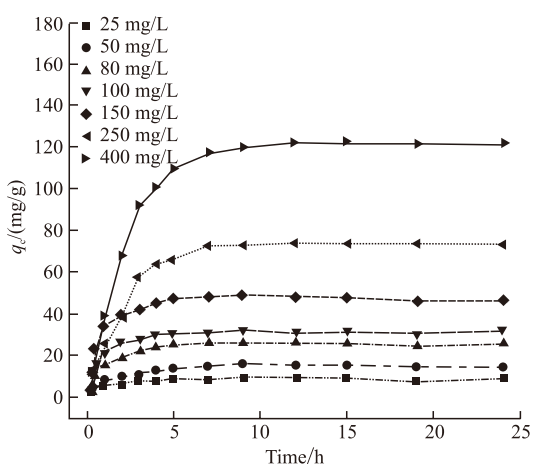


Fig.4 Effect of contact time at varying initial concentrations on TCP removal by CLDH

The effect of contact time (up to 24 h) at various initial concentrations (50-400 mg/L) of TCP was investigated at 25 °C. As depicted in Fig.4, the adsorption capacity of TCP increased with the contact time and attained equilibrium earlier for solutions with lower initial concentrations. At the initial contact time within 3 h, the adsorption of TCP occurred quickly, which may be due to the availability of a large number of vacant surface sites. The later slow rate of TCP adsorption is probably due to the electrostatic hindrance as well as the slow pore diffusion of the solute into the bulk of the adsorbent. And the equilibrium time became longer in higher initial TCP concentration solution. In this study, the adsorption equilibrium capacity increased from 8.63 to 122.04 mg/g with an increase in initial concentration from 30 to 400 mg/L. The high equilibrium adsorption capacity of TCP at initial concentration 400 mg/L may be explained in terms of the polarity of TCP and the mass transfer driving force. The TCP species have large polarity owing to large dipole moments of three chloro groups and hydroxyl

group (1.86 D and 1.69 D for chloro and hydroxyl, respectively). The polarity matching between CLDH and TCP is expected to result in the high adsorption capacity. In addition, the mass transfer driving force would become larger as the initial concentration increased, which could result in the higher TCP adsorption.

3.5 Effect of temperature

The effect of temperature on TCP uptake capacity (q_e) of CLDH was investigated at the adsorbent dose of 3 g/L and the results are given in Fig.5. It is shown that the TCP uptake capacity (q_e) increased with increasing temperature up to 55 °C, indicating that the adsorption of TCP was favored at higher temperatures. The adsorption of TCP is endothermic so that the extent of adsorption increased at higher temperature. In this study, all further experiments were carried out at 25 °C in an isothermal water bath shaker.

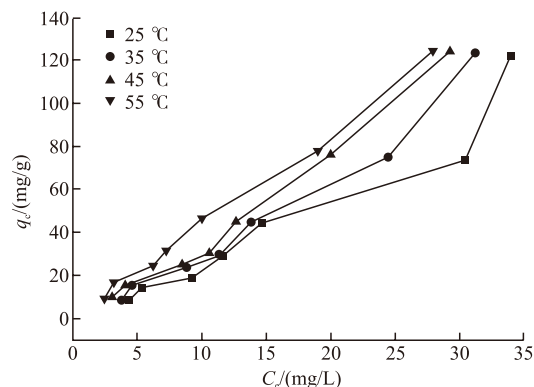


Fig.5 TCP adsorption on CLDH at various temperatures

3.6 Adsorption isotherm studies

The adsorption isotherm is to describe the adsorbate-adsorbent interactions in an adsorption system, and this information is essential in optimizing the use of adsorbents. For the liquid-solid system, adsorption isotherm equations commonly use the Langmuir equilibrium model, the Freundlich equilibrium model and the Tempkin equilibrium model. Langmuir's equation is based on the hypothesis that the maximum adsorption capacity consists of a monolayer on the free surface, and there is no interaction between adsorbed molecules. It is used for estimating the maximum uptake values which cannot be reached in the experiments. The empirical Freundlich model was chosen to estimate the adsorption capacity of the adsorbate on the adsorbent surface, which suited the non-ideal system. It is based on the fact that the adsorbent has a highly heterogeneous surface composed of different classes of adsorption sites. The Tempkin equilibrium model is based on the assumption

of multilayer adsorption, which considered the effects of some indirect adsorbent-adsorbate interactions on adsorption isotherms. The Langmuir equilibrium model (Eq.3), the empirical Freundlich model (Eq.4) and the Tempkin equilibrium model (Eq.5) can be described by the following linear forms of equations^[15,16]:

$$\frac{C_e}{q_e} = \frac{1}{K_L q_m} + \frac{C_e}{q_m} \quad (3)$$

where, K_L is the equilibrium adsorption coefficient ($L \cdot mg^{-1}$) and q_m the maximum adsorption capacity ($mg \cdot g^{-1}$), q_e is the amount adsorbed at equilibrium (mg/g).

$$\ln q_e = \ln K_f + \frac{1}{n} \ln C_e \quad (4)$$

where, K_f is the adsorption capacity at unit concentration, and n is adsorption intensity:

$$q_e = B_T \ln A + B_T \ln C_e \quad (5)$$

where, $B_T = (RT)/b$, T is the absolute temperature in Kelvin and R is the universal gas constant, $8.314 J/(mol \cdot K)$; A is the equilibrium binding constant ($L \cdot min^{-1}$) corresponding to the maximum binding energy.

Table 1 Freundlich, Langmuir and Tempkin isotherm parameters for the adsorption of TCP by CLDH

Thermodynamic model	$T/^\circ C$	Parameter		
		$k/(mg/g)$	n	R
Freundlich	25	1.934	0.994	0.9908
	35	2.196	1.109	0.9921
	45	2.652	1.110	0.9946
	55	4.407	0.994	0.9976
Langmuir		$Q_{max}/(mg/g)$	$K_L/(L/mg)$	
	25	353.4	0.00673	0.6999
	35	268.1	0.00963	0.6986
	45	289.9	0.01011	0.6190
	55	813.0	0.00374	0.4608
Tempkin		$B_T/(L/g)$	$A/(L/min)$	
	25	46.39	0.2185	0.909
	35	46.43	0.2486	0.916
	45	45.51	0.2852	0.906
	55	42.30	0.3917	0.939

All the correlation coefficient, R^2 values and the constants obtained from these three isotherm models applied for the adsorption of TCP onto CLDH at various temperatures are summarized in Table 1. It can be noticed that the Freundlich isotherm is a better model (correlation coefficient $R > 0.99$) than the Langmuir isotherm and the Temkin isotherms, whereas, the low correlation coefficients ($R < 0.80$) show poor agreement of the Langmuir isotherms with the experimental data, indicating the multilayer adsorption

on surface. The better fitting Freundlich parameters are shown in Table 1. The parameter n ($0.8826 < n < 1.0059$) in the Freundlich equation reveals adsorption sites with low energetical heterogeneity of this natural adsorbent. The constant n and K_f reached their corresponding maximum values with the highest correlation coefficient $R = 0.9976$ at 328 K, which implies that the binding capacity reached the highest value and the affinity between the adsorbent and TCP was also higher than those values investigated at other temperatures.

3.7 Thermodynamic of adsorption

Since the adsorption capacity depends on thermodynamic parameters, the adsorption process was assessed by the thermodynamic parameters such as the standard free energy change (ΔG^0), standard enthalpy change (ΔH^0) and standard entropy change (ΔS^0). The thermodynamic parameters were calculated using the following equations:

$$\Delta G^0 = -RT \ln K_f \quad (6)$$

$$\Delta G^0 = \Delta H^0 - T\Delta S^0 \quad (7)$$

Table 2 Gibbs free energy, enthalpy and entropy changes for the adsorption of TCP by Mg/Al-CLDH

$T/^\circ C$	$\Delta G^0/(kJ \cdot mol^{-1})$	$\Delta S^0/(J \cdot (mol \cdot K)^{-1})$	$\Delta H^0/(kJ \cdot mol^{-1})$
25	-1.635		
35	-2.014	77.94	21.83
45	-2.578		
55	-4.045		

The calculated values of thermodynamic parameters are shown in Table 2. The ΔG^0 values decrease from -1.635 to -4.045 kJ/mol when the temperature increases from 298 to 328 K, suggesting that a better adsorption occurred at higher temperatures. The negative values of ΔG^0 at different temperatures confirmed the feasibility and spontaneity of the adsorption of TCP onto CLDH. It is interesting to observe the positive values of ΔS^0 since there is a decrease in the freedom degree of the systems during the adsorption of TCP to the adsorbent. However, it should be noted that the reaction involves the release of the water of hydration from the TCP species and the surface of CLDH, which would lead to a positive value of ΔS^0 . And the positive values of ΔS^0 indicated that this structural change in adsorbate and adsorbent lead to a large positive ΔS^0 during the adsorption process. The positive values of ΔH^0 confirmed the endothermic nature of the adsorption process. When the value of ΔH^0 is smaller than 40 kJ/mol, it is the physisorption^[17]. Based on the given ΔH^0 , the adsorption of TCP onto

CLDH was a physisorption process. Similar results have been reported for the adsorption of other organic anions^[18,19].

3.8 Effect of temperature on kinetics

Since temperature is a highly significant parameter in the adsorption process, the kinetics for removal of TCP at different temperatures were studied and various kinetic models were applied to fit the experiment results: Lagergren's first order kinetic model (Eq.8), Ho's pseudo second order model (Eq. 9), and Chien's Elovich model (Eq.10).

The Lagergren's first order kinetic model and Ho's pseudo second order model in linear forms are expressed as^[20]:

$$\ln(q_e - q_t) = \ln q_e - k_1 t \quad (8)$$

$$\frac{t}{q_t} = \frac{1}{k_2 q_e^2} + \frac{t}{q_e} \quad (9)$$

where, k_1 and k_2 represent the rate constants of pseudo-first-order adsorption (min^{-1}) and pseudo-second-order adsorption ($\text{g}\cdot\text{mg}^{-1}\cdot\text{min}^{-1}$) respectively.

The kinetics of adsorption of TCP onto CLDH was also examined using Elovich equation:

$$q_t = \frac{1}{\beta} \ln \alpha \beta + \frac{1}{\beta} \ln t \quad (10)$$

where, α is the initial adsorption rate ($\text{mg}\cdot\text{g}^{-1}\cdot\text{min}^{-1}$), β is the desorption constant ($\text{g}\cdot\text{mg}^{-1}$) during any one experiment.

The parameters and the correlation coefficients are presented in Table 3. From the table, it can be seen that the pseudo-second-order kinetic model better represented the adsorption kinetics. The values of K_2 , $q_{e,\text{exp}}$ and $q_{e,\text{cal}}$ all increased with the temperature. Ozcan *et al*^[21] reported that the adsorption of Acid Blue 93 by natural sepiolite was physisorption, in which increasing the temperature increases the adsorption rate. And this result was in agreement with the thermodynamic analyses. The rate-limiting step of the adsorption would be discussed in the following section.

The adsorption rate constant k can be described by the well-known Arrhenius expression. The plot of the adsorption rate against the reciprocal temperature is depicted, giving a reasonable straight line ($R^2=0.992$). The slope (E_a/R) and activation energy (E_a) can be calculated from Arrhenius expression:

$$k = A e^{-(E_a/RT)} \quad (11)$$

The magnitude of activation energy gives an idea

about the type of adsorption which is mainly physical or chemical. For the diffusion-controlled process, the value of E_a is smaller than 20 kJ/mol ^[22]. The calculated E_a value, in our case, 2.087 kJ/mol , indicates that the process of TCP removal is controlled by the diffusion rather than the reaction between TCP and CLDH.

Table 3 Kinetics parameters for removal of TCP by Mg/Al-CLDH

Kinetic model	Parameter				
	$T/^\circ\text{C}$	$q_{e,\text{ex}}/(\text{mg/g})$	$q_{e,\text{cal}}/(\text{mg/g})$	$k_f/(\text{min}^{-1})$	R
Pseudo-first order	25	14.97	17.58	0.0079	0.995
	35	15.71	22.11	0.0113	0.985
	45	15.83	10.41	0.0122	0.988
	55	15.95	15.07	0.0209	0.986
Pseudo-second order	$T/^\circ\text{C}$	$q_{e,\text{ex}}/(\text{mg/g})$	$q_{e,\text{cal}}/(\text{mg/g})$	$k_f/(\text{min}^{-1})$	R
	25	14.97	14.02	1.123	0.996
	35	15.71	14.02	2.322	0.997
	45	15.83	14.49	4.322	0.998
55	15.95	15.37	7.679	0.998	
Elovich model	$T/^\circ\text{C}$	$\alpha/(\text{mg}\cdot\text{g}^{-1}\cdot\text{min}^{-1})$	$\beta/(\text{mg}\cdot\text{g}^{-1})$	R	
	25	174.7	0.48031	0.887	
	35	398.7	0.54377	0.864	
	45	1588	0.63452	0.856	
55	65144	0.91158	0.765		
Intra-particle diffusion	$C_i/(\text{mg/g})$	$k/(\text{mg}\cdot\text{g}^{-1}\cdot\text{h}^{-0.5})$	$C/(\text{mg/g})$	R	
	30	3.31	1.46	0.985	
	50	4.44	3.72	0.992	
	80	8.45	6.99	0.993	
	100	8.54	12.98	0.979	
	150	10.12	24.61	0.995	
250	15.82	31.01	0.996		
400	27.79	44.82	0.984		

3.9 Adsorption mechanism

Typically, various mechanisms control the adsorption kinetics and the predominating mechanism is the diffusion mechanism, including external diffusion, boundary layer diffusion and intraparticle diffusion^[23]. In order to study the mechanism and rate-controlling steps affecting the kinetics of adsorption, the experimental data were further processed in this work. The intraparticle diffusion model was tested, and an intra-particle diffusion coefficient k_p ($\text{mg}\cdot\text{g}^{-1}\cdot\text{h}^{-0.5}$) is defined by the equation^[24]:

$$q_t = k_p \times t^{1/2} + C \quad (12)$$

The relationships between q_t and $t^{1/2}$ at various initial concentrations ($50\text{-}400 \text{ mg}\cdot\text{L}^{-1}$) TCP are given in Fig.6. As can be seen from Fig. 6, the plots of different initial concentrations show similar features that the plot obtained consists of three straight lines, and similar results could be found in the reported Ref.[25]. In addition, the plots were not linear over the whole time range, implying that more than one processes affected the adsorption, which contains both

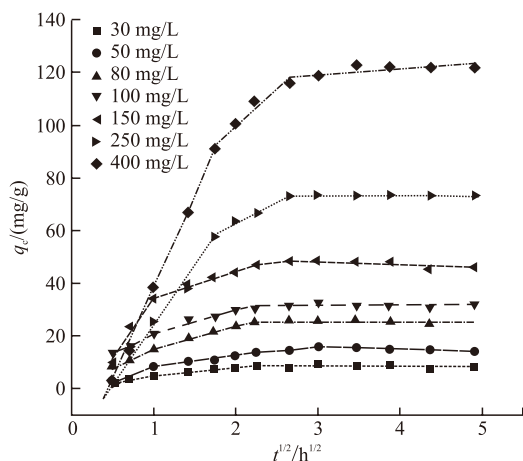


Fig.6 Intra-particle diffusion plots for the TCP removal by CLDH

the surface adsorption and intraparticle diffusion. The first linear section can be attributed to the diffusion of adsorbate through the solution and the boundary layer to the external surface of adsorbent. In the linear second section, plots do not pass through the origin, which suggests that the intraparticle diffusion is not the rate-limiting step, but some degree of boundary layer control. After two linear segments, the last plateau section described the final equilibrium for which the intraparticle diffusion started to slow down. However, it can be noticed that the slopes of the first linear section and the second linear section were increased with an increase in initial concentration, respectively. The slope of the linear portion indicated the rate of the adsorption. The lower slope corresponded to a slower adsorption process. The increase of slope can be explained by the increase of the mass transfer driving force. And the constants of k_p and C for the second linear section are shown in Table 3. From the table, it can be noticed that the intraparticle diffusion coefficient k_p for the diffusion in the second region is increased from 3.31 to 27.79 $\text{mg}\cdot\text{g}^{-1}\cdot\text{h}^{-0.5}$ with an increase in initial concentration. The value of the intercept C in this second section provides information related to the thickness of the boundary layer, which increased with increasing initial concentration. The increase of the intercept C suggests that increasing the TCP concentration of the solution would increase the rate of diffusion of TCP in the boundary layer. In other words, the surface diffusion became more important at high concentration. Similar results could be found in the reported literatures^[19,26].

4 Conclusions

The results of this study indicated that calcined $\text{Mg}/\text{Al}-\text{CO}_3$ layered double hydroxide may potentially

be employed as an adsorbent in the removal of TCP (94.7% of removal percentage in initial TCP concentration 50 mg/L, CLDH dose 3 g/L). The kinetics of adsorption was shown to be suitably described by the pseudo-second-order kinetics model, and the calculated value of E_a was $2.087 \text{ kJ}\cdot\text{mol}^{-1}$, indicating that diffusion controlled the process of TCP removal. The thermodynamic analysis presented that the processes of adsorption were endothermic, spontaneous and entropy-gained nature of the process. The Freundlich isotherm model obtained well fitted the experimental data. With the supports of characterization by several techniques and thermodynamic analysis, the adsorption is a physical adsorption process. The intraparticle diffusion model showed that increasing the TCP concentration of the solution would increase the rate of diffusion of TCP in the boundary layer, and the overall rate of adsorption can be described by three steps: surface diffusion, particle diffusion and diffusion equilibrium.

References

- [1] Jiang M, Niu SQ, Zhan HY, *et al.* Research Advances in Biodegradation of Chlorophenols in Environment[J]. *Chinese Journal of Applied Ecology*, 2003, 14(6): 1 003-1 006
- [2] Nikolaou AD, Kostopoulou MN, Lekkas TD. Organic By-products of Drinking Water Chlorination[J]. *Global NEST: The International Journal*, 1999, 1(3): 143-156
- [3] Fingler S, Dravenkar V. Chlorophenols in the Sava River before, in and after the Zagreb City Area. Impact on the Purity of the City Ground and Drinking Waters[J]. *Toxicol. Environ. Chem.*, 1988, 17: 319-328
- [4] Chen GC, Shan XQ, Wang YS, *et al.* Adsorption of 2,4,6-Trichlorophenol by Multi-walled Carbon Nanotubes as Affected by Cu(II) [J]. *Water Res.*, 2009, 43: 2 409-2 418
- [5] Tan IA, Ahmad AL, Hameed BH. Adsorption Isotherms, Kinetics, Thermodynamics and Desorption Studies of 2,4,6-Trichlorophenol on Oil Palm Empty Fruit Bunch-based Activated Carbon[J]. *J. Hazard. Mater.*, 2009, 164: 473-482
- [6] Eker S, Kargi F. Biological Treatment of 2,4,6-Trichlorophenol (TCP) Containing Wastewater in a Hybrid Bioreactor System with Effluent Recycle[J]. *J. Environ. Manage.*, 2009, 90 (2), 692-698
- [7] Konyantinos CC, Eleni S, Maria L, *et al.* Mechanism of Catalytic Degradation of 2,4,6-Trichlorophenol by a Fe-porphyrin Catalyst[J]. *Appl. Catal. B-Environ.*, 2011, 101: 417-424
- [8] Gaya UI, Abdullah AH, Hussein M Z, *et al.* Photocatalytic Removal of 2,4,6-Trichlorophenol from Water Exploiting Commercial ZnO Powder[J]. *Desalination*, 2010, 263: 176-182
- [9] Bulut Y, Gozubenli N, Aydin H. Equilibrium and Kinetics Studies for Adsorption of Direct Blue 71 from Aqueous Solution by Wheat Shells[J]. *J. Hazard. Mater.*, 2007, 144: 300-306

- [10] Wang XP, Shan XQ, Luo L, et al. Sorption of 2,4,6-Trichlorophenol in Model Humic Acid-clay Systems[J]. *J. Agric. Food. Chem.*, 2005, 53: 3 548-3 555
- [11] Goh KH, Lim TT, Dong ZL. Application of Layered Double Hydroxides for Removal of Oxyanions: A Review[J]. *Water Res.*, 2008, 42: 1 343-1 368
- [12] Turk T, Aip I, Deveci H. Adsorption of As(V) from Water Using Mg-Fe-based Hydrotalcite (FeHT)[J]. *J. Hazard. Mater.*, 2009, 171: 665-670
- [13] Angeles M, Gabriela JA, Getsemani MM, et al. Photoassisted Degradation of 4-Chlorophenol and p-Cresol Using MgAl Hydrotalcites[J]. *Ind. Eng. Chem.Res.*, 2011, 50: 2 762-2 767
- [14] Iyi N, Sasaki T. Deintercalation of Carbonate Ions and Anion Exchange of an Al-rich MgAl-LDH (Layered Double Hydroxide)[J]. *Appl. Clay. Sci.*, 2008, 42: 246-251
- [15] Kavitha D, Namasivayam C. Experimental and Kinetic Studies on Methylene Blue Adsorption by Coir Pith Carbon[J]. *Bioresour. Technol.*, 2007, 98: 14-21
- [16] Tseng RL, Wu FC. Inferring the Favorable Adsorption Level and the Concurrent Multi-stage Process with the Freundlich Constant[J]. *J. Hazard. Mater.*, 2008, 155(1-2): 277-287
- [17] Karam, Yuzer H, Sabah E, et al. Adsorption of Cobalt from Aqueous Solutions onto Sepiolite[J]. *Water Res.*, 2003, 37 (1): 224-232
- [18] Li KQ, Zheng Z, Huang XF, et al. Equilibrium, Kinetic and Thermodynamic Studies on the Adsorption of 2-Nitroaniline onto Activated Carbon Prepared from Cotton Stalk Fibre[J]. *J. Hazard. Mater.*, 2009, 166: 213-220
- [19] Zaghouane-Boudiafa H, Boutahala M, Tiar C, et al. Treatment of 2,4,5-Trichlorophenol by MgAl-SDBS organo-layered Double Hydroxides: Kinetic and Equilibrium Studies[J]. *Chem. Eng. J.*, 2011, 173(1): 36-414
- [20] Ho YS, Mckay GA. Comparison of Chemisorption Kinetic Models Applied to Pollutant Removal on Various Sorbents[J]. *Process Saf. Environ. Prot.*, 1998, 76: 332-340
- [21] Ozcan A, Oncu EM, Ozcan AS. Kinetics, Isotherm and Thermodynamic of Adsorption of Acid Blue 193 from Aqueous Solutions onto Natural Sepiolite[J]. *Colloids Surf. A*, 2006, 277: 90-97
- [22] Ho YS, Ng JCY, Mckay G. Kinetics of Polutant Sorption by Biosorbents: Review[J]. *Sep. Purif. Methods*, 2000, 29: 189-232
- [23] Guibal E, Mccarrick P, Tobin JM. Comparison of the Adsorption of Anionic Dyes on Activated Carbon and Chitosan Derivatives from Dilute Solutions[J]. *Sep. Sci. Technol.*, 2003, 38: 3 049-3 073
- [24] Mckay G, Otterburn MS, Sweeney AG. The Removal of Colour from Effluent Using Various Adsorbents-III Silica: Rate Processes[J]. *Sweeney. Water Res.*, 1980, 14 (152): 11-20
- [25] Liu W, Li LQ, Yao XL, et al. Role of Pore Structure of Activated Carbon in Adsorption for Acetone[J]. *Journal of Central South University: Science and Technology*, 2012, 43 (4): 1 574-1 583 (in Chinese)
- [26] Lazaridis NK, Asouhidou DD. Kinetics of Sorptive Removal of Chromium(VI) from Aqueous Solutions by Calcined Mg-Al-CO₃ Hydrotalcite[J]. *Water Res.*, 2003, 37: 2 875-2 882